Accretion and Accretion Disks

Introduction

AGN are powered by accretion $\Longrightarrow$ need to look at accretion as a physical mechanism.

Unfortunately, this will have to be somewhat theoretical, but this cannot be avoided...

Structure of this chapter:

1. Accretion Luminosity: Eddington luminosity
2. Accretion Disks: Theory
3. Accretion Disks: Confrontation with observations

Literature

- J. Frank, A. King, D. Raine, 2002, Accretion Power in Astrophysics, 3rd edition, Cambridge Univ. Press

  The standard textbook on accretion, covering all relevant areas of the field.

- T. Padmanabhan, 2001, Theoretical Astrophysics, II. Stars and Stellar Systems, Cambridge Univ. Press

  See introduction to this lecture.

- N.I. Shakura & R. Sunyaev, 1973, Black Holes in Binary Systems. Observational Appearance. Astron. Astrophys. **24**, 337

  The fundamental paper, which *really* started the field.

- J.E. Pringle, 1981, Accretion Disks in Astrophysics, Ann. Rev. Astron. Astrophys. **19**, 137

  Concise review of classical accretion disk theory.

Eddington luminosity

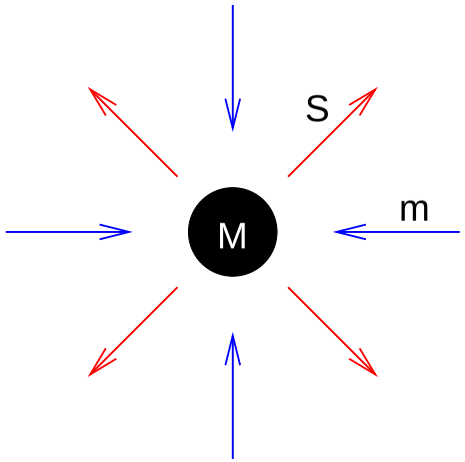

Assume mass M spherically symmetrically accreting ionized hydrogen gas.
At radius r, accretion produces energy flux S.
Important: Interaction between accreted material and radiation!

Eddington luminosity

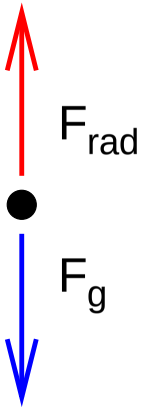

Force balance on accreted electrons and protons:
Inward force: gravitation:

$$F_\mathrm{g} = \frac{GMm_\mathrm{p}}{r^2} \tag{4.5}$$

Outward force: radiation force:

$$F_\mathrm{rad} = \frac{\sigma_\mathrm{T} S}{c} \tag{4.6}$$

where energy flux S is given by

$$S = \frac{L}{4\pi r^2} \tag{4.7}$$

where L: luminosity.
Note: $\sigma_\mathrm{T} \propto (m_\mathrm{e}/m_\mathrm{p})^2$, so negligable for protons.
But: strong Coulomb coupling between electrons and protons $\Longrightarrow$ F_rad also has effect on protons!

Eddington luminosity

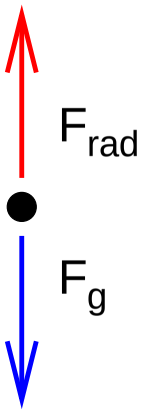

Accretion is only possible if gravitation dominates:

$$\frac{GMm_\mathrm{p}}{r^2} > \frac{\sigma_\mathrm{T} S}{c} = \frac{\sigma_\mathrm{T}}{c} \cdot \frac{L}{4\pi r^2} \tag{4.8}$$

and therefore

$$L < L_\mathrm{Edd} = \frac{4\pi GMm_\mathrm{p} c}{\sigma_\mathrm{T}} \tag{4.9}$$

or, in astronomically meaningful units

$$L < 1.3 \times 10^{38}\,\mathrm{erg\,s^{-1}} \cdot \frac{M}{M_\odot} \tag{4.10}$$

where L_Edd is called the Eddington luminosity.

But remember the assumptions entering the derivation: spherically symmetric accretion of fully ionized pure hydrogen gas.

Eddington luminosity

Characterize accretion process through the accretion efficiency, η:

$$L = \eta \cdot \dot{M} c^2 \tag{4.11}$$

where $\dot{M}$: mass accretion rate (e.g., $\mathrm{g\,s^{-1}}$ or $M_\odot\,\mathrm{yr^{-1}}$).

Therefore maximum accretion rate ("Eddington rate"):

$$\dot{m} = \frac{L_\mathrm{Edd}}{\eta c^2} \sim 2 \cdot \left(\frac{M}{10^8\,M_\odot}\right) M_\odot\,\mathrm{yr^{-1}} \tag{4.12}$$

(for $\eta = 0.1$)

Emitted spectrum

Characterize photon by its radiation temperature, T_rad:

$$h\nu \sim kT_\mathrm{rad} \quad \Longrightarrow \quad T_\mathrm{rad} = h\nu/k \tag{4.19}$$

Optically thick medium: blackbody radiation

$$T_\mathrm{b} = \left(\frac{L}{4\pi R^2 \sigma_\mathrm{SB}}\right)^{1/4} \tag{4.20}$$

Optically thin medium: L directly converted into radiation without further interactions $\Longrightarrow$ mean particle energy

$$T_\mathrm{th} = \frac{GMm_\mathrm{p}}{3kR} \tag{4.21}$$

Plugging in numbers for a typical solar mass compact object (NS/BH):

$$T_\mathrm{rad} \sim 1\,\mathrm{keV} \quad \text{and} \quad T_\mathrm{bb} \sim 50\,\mathrm{MeV} \tag{4.22}$$

Accreting objects are broadband emitters in the X-rays and gamma-rays.

CXC/MPE/S. Komossa

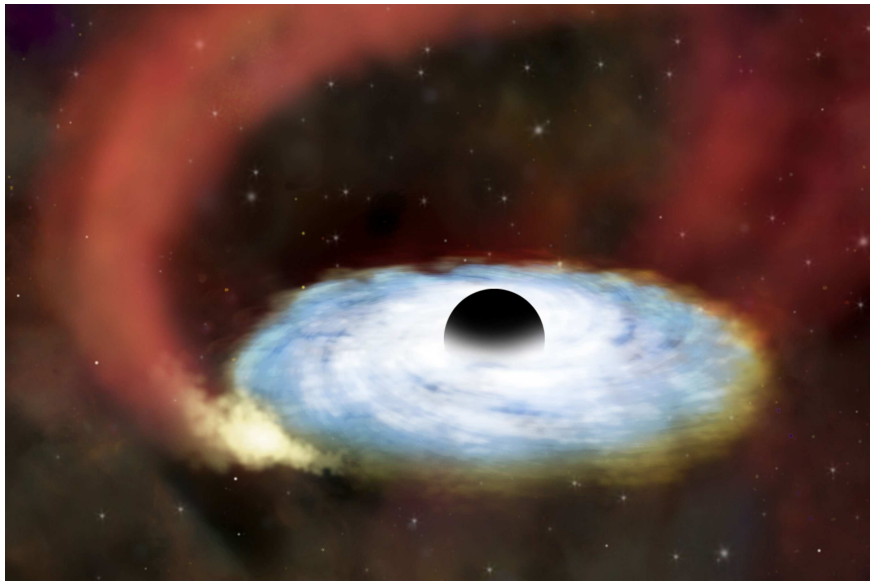

NASA/CXC/SAO

Source of matter: probably disrupted stars

$\Longrightarrow$ accreted matter has angular momentum

$\Longrightarrow$ accretion disk forms.

Thin Disks

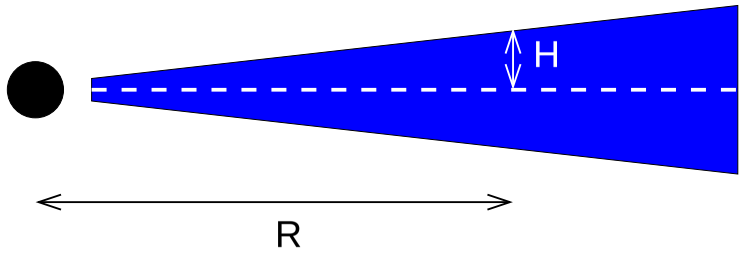

Most important case: thin accretion disks, i.e., vertical thickness, H, much smaller than radius R:

$$H \ll R \tag{4.23}$$

$\Longrightarrow$ Requires that radiation pressure is negligable

$\Longrightarrow L \ll L_{\text{Edd}}$

Thin Disks

Will calculate disk structure in exercises, here we'll only look at most important parameter: temperature profile.

Assume angular velocity of particles in disk $\gg$ radial motion

$\Longrightarrow$ Kepler motion.

$$v_r = \sqrt{\frac{GM}{r}} \tag{4.24}$$

Total specific energy of particles at distance r:

$$\epsilon_{\text{spec}} = \frac{E_{\text{tot}}(r)}{m} = -\frac{GM}{r} + \frac{1}{2}\frac{GM}{r} = -\frac{GM}{2r} \tag{4.25}$$

Energy lost when matter moves from $r + dr \rightarrow r$:

$$\Delta\epsilon_{\text{spec}} = \frac{dE(r)}{dr}\,dr = -\frac{GM}{2r^2}\,dr \tag{4.26}$$

This energy is radiated away. For a ring in an optically thick disk:

$$dE = \sigma T^4 \cdot 2\pi r\,dr \propto -\frac{GM}{2r^2}\,dr \quad \Longrightarrow \quad T(r) \propto r^{-3/4} \tag{4.27}$$

Thin Disks

Basic exact results for thin disks (see exercises for details!):

$$T(R) = \left\{ \frac{3GM\dot{M}}{8\pi R^3 \sigma_{\rm SB}} \left[1 - \left(\frac{R_*}{R} \right)^{1/2} \right] \right\}^{1/4}$$
$$= 6.8 \times 10^5\,{\rm K} \cdot \eta^{-1/4} \left(\frac{L}{L_{\rm Edd}} \right)^{1/2} L_{46}^{-1/4} \mathcal{R}^{1/4} x^{-3/4}$$

where $\eta = L_{\rm Edd}/\dot{M}_{\rm Edd}c^2$, $x = c^2 R/2GM$, $\mathcal{R} = (1 - (R_*/R)^{1/2})$.

Radial dependence of T:

$$T(R) \propto R^{-3/4}$$

Dependence on mass (note: for NS/BH inner radius $R_* \propto M$!):

$$T_{\rm in} \propto (\dot{M}/M^2)^{1/4}$$

$\Longrightarrow$ AGN disks are colder than disks around galactic BH

Thin Disks: Emitted Spectrum

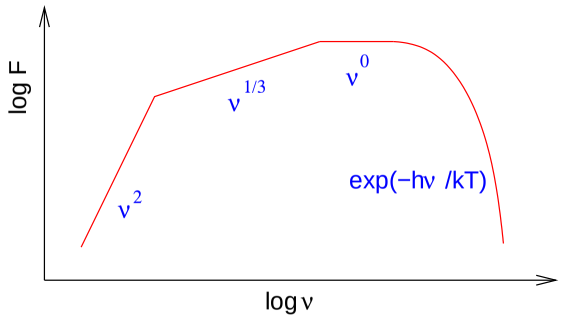

If disk is optically thick, then locally emitted spectrum is a black body, $B_\nu(T(r))$.

Total emitted spectrum obtained by integrating over disk

$$F_\nu = \int_{R_*}^{R_{\rm out}} B_\nu(T(R))\, 2\pi R\, dR \qquad (4.28)$$

The resulting spectrum looks essentially like a stretched black body.

Thin Disks: Emitted Spectrum

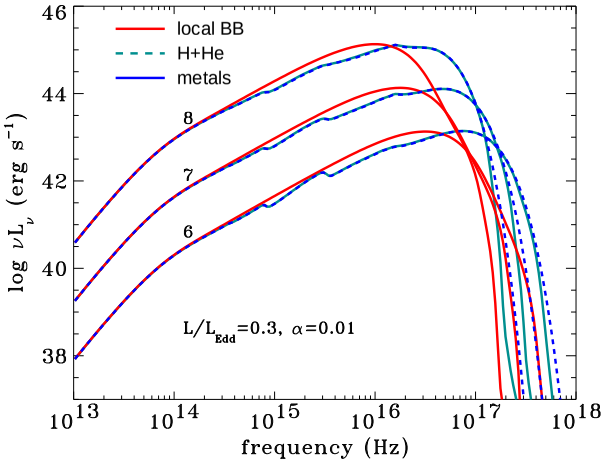

Hubeny et al., 2001, Fig. 13

In reality: accretion disk spectrum depends on

- elemental composition ("metallicity")
- viscosity ("α-parameter")
- ionization state and luminosity of disk ($\dot{M}$)
- properties of compact object

and many further parameters

Until today: no really satisfactory disk model available.

Thin Disks: Emitted Spectrum

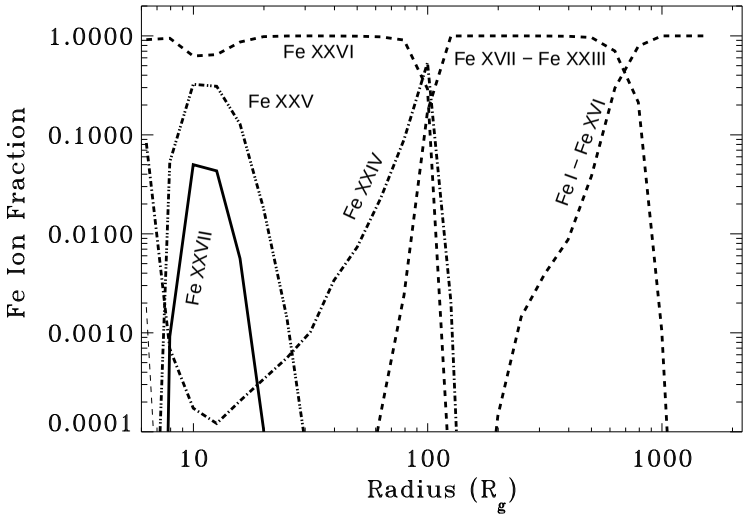

Fe species in a disk around a Galactic BH (Davis et al., 2005, Fig. 6)

Viscosity

Most important unknown in accretion disk theory: viscosity

even though it dropped out of $T(R)$!

Earth: viscosity of fluids typically due to molecular interactions (molecular viscosity).

Kinematic viscosity:

$$\nu_{\rm mol} \sim \lambda_{\rm mfp} c_{\rm s} \tag{4.29}$$

where the mean free path

$$\lambda_{\rm mfp} \sim \frac{1}{n\sigma} \sim 6.4 \times 10^4 \left(\frac{T^2}{n}\right) \ {\rm cm} \tag{4.30}$$

and the speed of sound

$$c_{\rm s} \sim 10^4 T^{1/2} \, {\rm cm \, s^{-1}} \tag{4.31}$$

such that

$$\nu_{\rm mol} \sim 6.4 \times 10^8 \, T^{5/2} n^{-1} \, {\rm cm^2 \, s^{-1}} \tag{4.32}$$

Viscosity

Viscosity is important for small Reynolds numbers ("laminar flow"), where

$$\mathrm{Re} = \frac{\text{inertial force}}{\text{viscous force}} \sim \frac{\rho R v}{\rho \nu} = \frac{R v}{\nu} \tag{4.33}$$

Follows from Navier-Stokes Equations

Using typical accretion disk parameters:

$$\mathrm{Re}_{\rm mol} \sim 2 \times 10^{14} \left(\frac{M}{M_\odot}\right)^{1/2} \left(\frac{R}{10^{10} \, {\rm cm}}\right)^{1/2} \left(\frac{n}{10^{15} \, {\rm cm^{-3}}}\right) \left(\frac{T}{10^4 \, {\rm K}}\right)^{-5/2} \tag{4.34}$$

$\Longrightarrow$ Molecular viscosity is irrelevant for astrophysical disks!

since $\mathrm{Re} \gtrsim 10^3$: turbulence $\Longrightarrow$ Shakura & Sunyaev posit turbulent viscosity

$$\nu_{\rm turb} \sim v_{\rm turb} \ell_{\rm turb} \sim \alpha \, c_{\rm s} \cdot H \tag{4.35}$$

where $\alpha \lesssim 1$ and $\ell_{\rm turb} \lesssim H$ typical size for turbulent eddies.

Viscosity

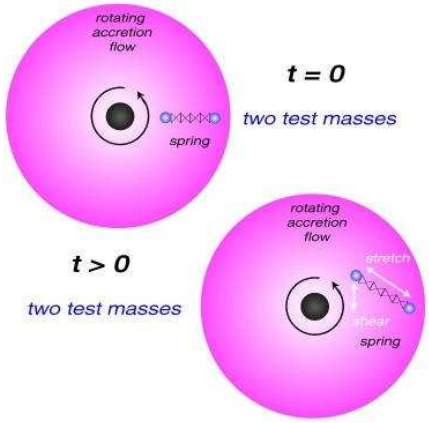

R. Müller

Mechanical analogy of MRI: spring in differentially rotating medium.

Physics of turbulent viscosity is unknown, however, α prescription yields good agreement between theory and observations.

Possible origin: Magnetorotational instability (MRI): MHD instability amplifying B-field inhomogeneities caused by small initial radial displacements in accretion disk $\Longrightarrow$ angular momentum transport

(Balbus & Hawley 1991, going back to Velikhov 1959 and Chandrasekhar (1961).

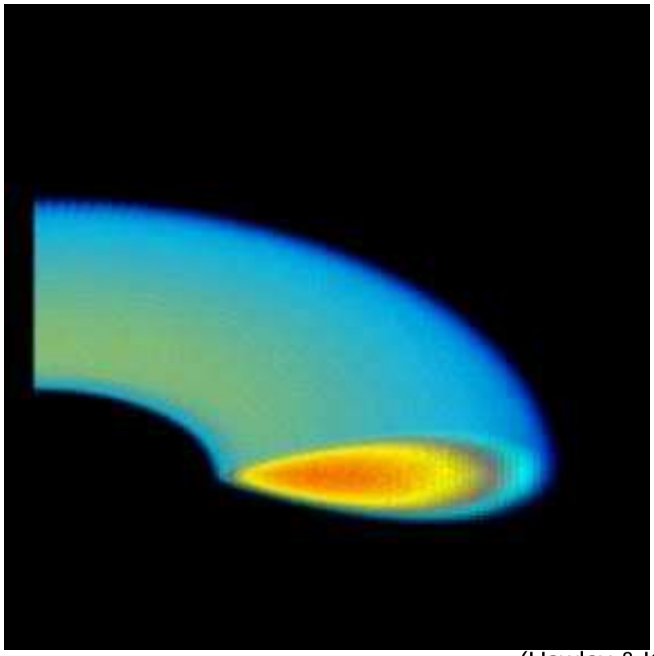

(Hawley & Krolik, 2002)

Accretion Disks in AGN

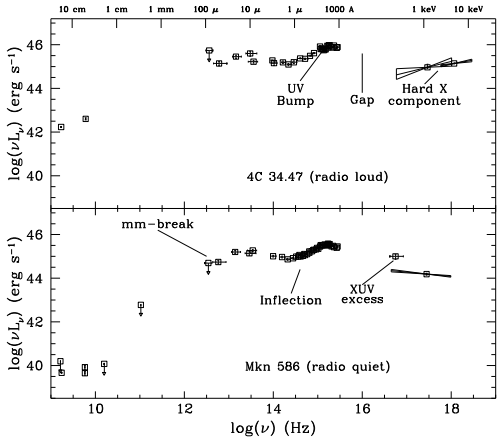

Spectral Energy Distribution of radio-loud and radio-quiet AGN (Elvis et al., 1994)

Big Blue Bump: Excess radiation in ∼UV range $\Longrightarrow$ disk?

IR Bump: Excess radiation in ∼IR range $\Longrightarrow$ dust? (peak T: 2000 K; dust sublimation?)

Accretion Disks in AGN

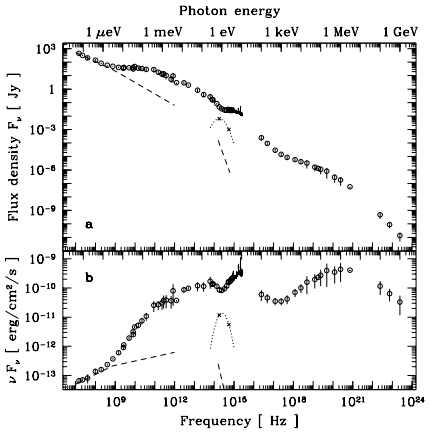

Spectral Energy Distribution of 3C273 (Türler et al., 1999)

Big Blue Bump: Excess radiation in ∼UV range $\Longrightarrow$ disk?

IR Bump: Excess radiation in ∼IR range $\Longrightarrow$ dust? (peak T: 2000 K; dust sublimation?)

IR Bump

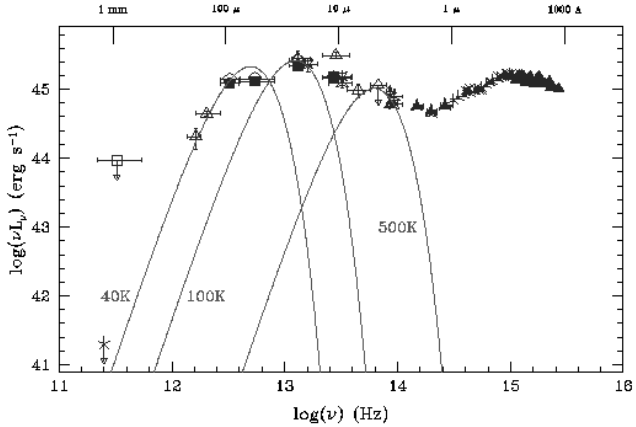

mm–optical SED of PG1351+640: dust has wide range of temperatures (Wilkes, 2004).

IR-Bump: too cold for disk, has substructure $\Longrightarrow$ different emission regions.

UV Bump

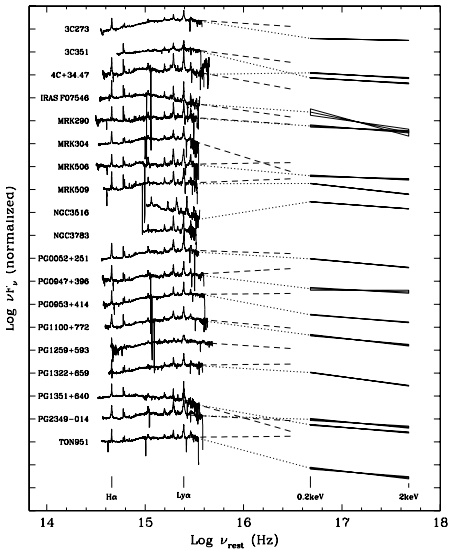

In *some* AGN: extrapolated UV power law smoothly matches the X-ray continuum.

Remember: $f_\nu \propto \nu^{-\alpha}$

Break wavelengh between 800 and 1600 Å, in rough agreement with accretion disk models.

Theory of the break: H-Lyman edge, possibly smeared by Comptonization or relativistic effects.

However: no correlation between UV slope and BH mass as expected from accretion disk models?!?

(Shang et al., 2005)

Galactic Black Holes

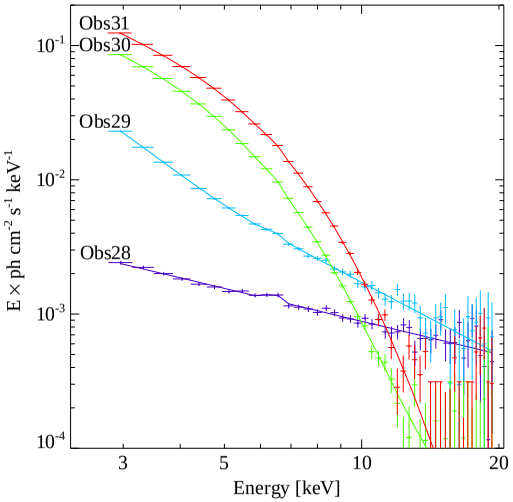

LMC X-3, (Wilms et al., 2001)

Problem with AGN: peak of disk in UV

$\Longrightarrow$ Galactic Black Holes: T is higher

Find ok agreement between accretion disk models and theory.

In general: models with just $T \propto r^{-3/4}$ and no additional (atomic) physics seem to work best?!?

Balbus, S. A., & Hawley, J. F., 1991, ApJ, 376, 214

Chandrasekhar, S., 1961, Hydrodynamic and Hydromagnetic Stability, (Oxford: Oxford Univ. Press), (reprinted 1981 by Dover, New York)

Davis, S. W., Blaes, O. M., Hubeny, I., & Turner, N. J., 2005, ApJ, 621, 372

Davis, S. W., Done, C., & Blaes, O. M., 2006, ApJ, 647, 525

Elvis, M., et al., 1994, ApJS, 95, 1

Hawley, J. F., & Krolik, J. H., 2002, ApJ, 566, 164

Shang, Z., et al., 2005, ApJ, 619, 41

Türler, M., et al., 1999, A&AS, 134, 89

Velikhov, E. P., 1959, Sov. Phys. – JETP, 9, 995

Wilkes, B., 2004, in AGN Physics with the Sloan Digital Sky Survey, ed. G. T. Richards, P. B. Hall, 37

Wilms, J., Nowak, M. A., Pottschmidt, K., Heindl, W. A., Dove, J. B., & Begelman, M. C., 2001, MNRAS, 320, 327

Galactic Black Holes

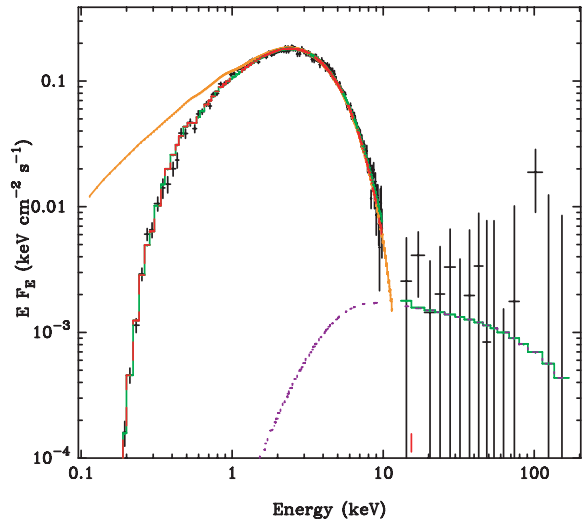

(Davis, Done & Blaes, 2006)

Comparison of self-consistent accretion disk model with LMC X-3 data $\Longrightarrow$ good agreement, although values of α smaller than expected (fits find $0.01 < \alpha < 0.1$ instead of 0.1–0.8).

Top red line: inferred accretion disk spectrum without interstellar absorption.

X-Ray Detectors

Introduction

A large amount of our understanding of AGN comes from non-optical observations.

$\Longrightarrow$ we need to understand how these observations are made to be able to interpret their results.

$\Longrightarrow$ Will take a “side trip” into the world of X-ray detectors.

There are two main issues to deal with:

- X-ray Optics
- X-ray Detectors

Earth’s Atmosphere

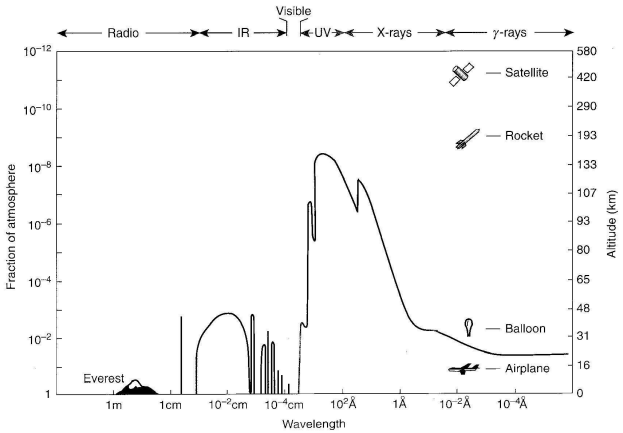

Charles & Seward, Fig. 1.12

Earth’s atmosphere is opaque for all types of EM radiation except for optical light and radio.

Major contributer at high energies: photoabsorption ($\propto E^{-3}$), esp. from oxygen (edge at $\sim$500 eV).

$\Longrightarrow$ If one wants to look at the sky in other wavebands, one *has* to go to space!

Optical Imaging

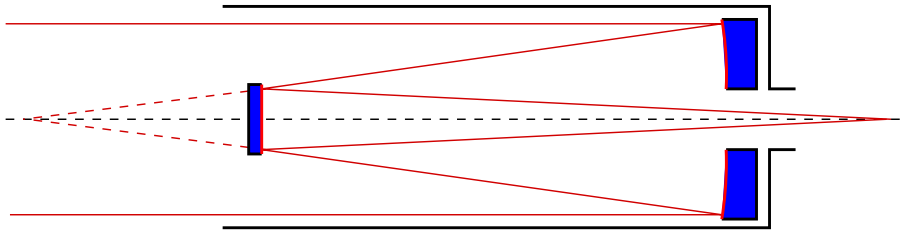

Cassegrain telescope, after Wikipedia

Reminder: Optical telescopes are usually reflectors:

primary mirror (paraboloid) $\rightarrow$ secondary mirror (often flat) $\rightarrow$ detector

Main characteristics of a telescope:

- collecting area (i.e., open area of telescope, $\sim \pi d^2/4$, where d: telescope diameter)
- for small telescopes: angular resolution,

$$\theta = 1.22 \frac{\lambda}{d} \qquad (5.1)$$

but in the optical: do not forget the seeing!

Optical Imaging

Optical telescopes are based on principle that reflection “just works” with metallic surfaces.

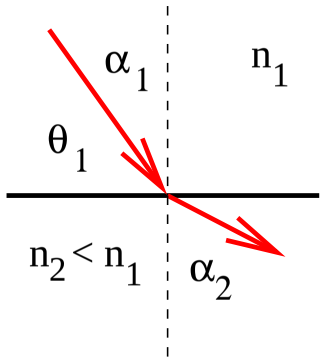

Snell’s law of refraction:

$$\frac{\sin\alpha_1}{\sin\alpha_2} = \frac{n_2}{n_1} = n \qquad (5.2)$$

where n index of refraction, and $\alpha_{1,2}$ angle wrt. surface normal. If $n \gg 1$: Total internal reflection

Total reflection occurs for $\alpha_2 = 90°$, i.e. for

$$\sin\alpha_{1,c} = n \quad \Longleftrightarrow \quad \cos\theta_c = n \qquad (5.3)$$

with the critical angle $\theta_c = \pi/2 - \alpha_{1,c}$.
Clearly, total reflection is only possible for $n < 1$.

Light in glass at glass/air interface: $n = 1/1.6 \Longrightarrow \theta_c \sim 50° \Longrightarrow$ principle behind optical fibers.

Optical Imaging

In general, the index of refraction is given by the Maxwell relation,

$$n = \sqrt{\epsilon\mu} \qquad (5.4)$$

where ϵ is the dielectricity constant and where $\mu \sim 1$ is the permeability of the material.

For free electrons (e.g., in a metal), Jackson (1975, eq. 7.59) shows that

$$\epsilon = 1 - \left(\frac{\omega_p}{\omega}\right)^2 \quad \text{with} \quad \omega_p^2 = \frac{4\pi n Z e^2}{m_e} \qquad (5.5)$$

where ω_p is called the plasma frequency and where n is the number density of atoms and Z is the nuclear charge.
(i.e., nZ is the number density of electrons)

With $\omega = 2\pi\nu = 2\pi c/\lambda$, Eq. (5.5) becomes

$$\epsilon = 1 - \frac{nZe^2}{\pi m_e c^2}\lambda^2 = 1 - \frac{nZr_e}{\pi}\lambda^2 \qquad (5.6)$$

$r_e = e^2/m_e c^2 \sim 2.8 \times 10^{-13}$ cm is the classical electron radius.

Optical Imaging

$$n = \sqrt{1 - \frac{nZr_e}{\pi}\lambda^2} \sim 1 - \frac{nZr_e}{2\pi}\lambda^2 = 1 - \frac{\rho}{(Z/A)m_u}\frac{r_e}{2\pi}\lambda^2 =: 1 - \delta \qquad (5.7)$$

Z: atomic number, A: atomic weight ($Z/A \sim 0.5$), ρ: density, $m_u = 1$ amu $= 1.66 \times 10^{-24}$ g

Critical angle for X-ray reflection:

$$\cos\theta_c = 1 - \delta \qquad (5.8)$$

Since $\delta \ll 1$, Taylor ($\cos x \sim 1 - x^2/2$):

$$\theta_c = \sqrt{2\delta} = 5.6' \left(\frac{\rho}{1\,\mathrm{g\,cm^{-3}}}\right)^{1/2} \frac{\lambda}{1\,\mathrm{nm}} \qquad (5.9)$$

So for $\lambda \sim 1$ nm: $\theta_c \sim 1°$.

Optical Imaging

Typical parameters for selected elements

	Z	ρ	nZ
		g cm^{-3}	e$^-$ Å^{-3}
C	6	2.26	0.680
Si	14	2.33	0.699
Ag	47	10.50	2.755
W	74	19.30	4.678
Au	79	19.32	4.666

After Als-Nielsen & McMorrow (Tab. 3.1)

To increase θ_c: need material with high ρ

$\Longrightarrow$ gold (*XMM-Newton*) or iridium (*Chandra*).

For more information on mirrors etc., see, e.g., Aschenbach, 1985, Rep Prog Phys 48, 579, or Als-Nielsen & McMorrow, 2004, Elements of Modern X-ray Physics, Wiley

Optical Imaging

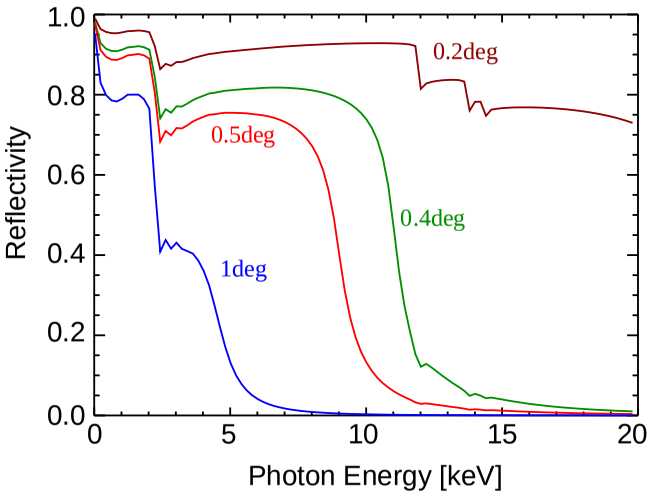

Reflectivity for Gold

X-rays: Total reflection only works in the soft X-rays and only under grazing incidence $\Longrightarrow$ grazing incidence optics.

Wolter Telescopes

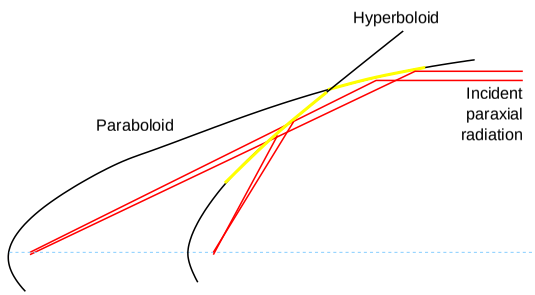

To obtain manageable focal lengths ($\sim$ 10 m), do imaging with telescope using two reflections on a parabolic and a hyperboloidal mirror ("Wolter type I").

(Wolter, 1952, for X-ray microscopes, Giacconi, 1961, for UV- and X-rays).

But: small collecting area ($A \sim \pi r^2 l/f$ where f: focal length)

Wolter Telescopes

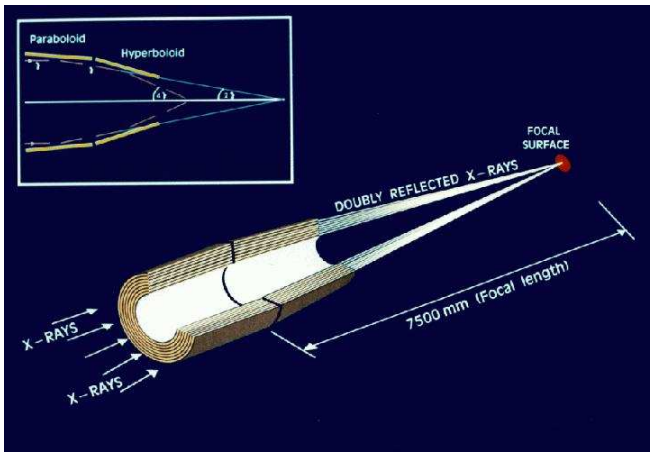

ESA/XMM

Solution to small collecting area: nested mirrors.

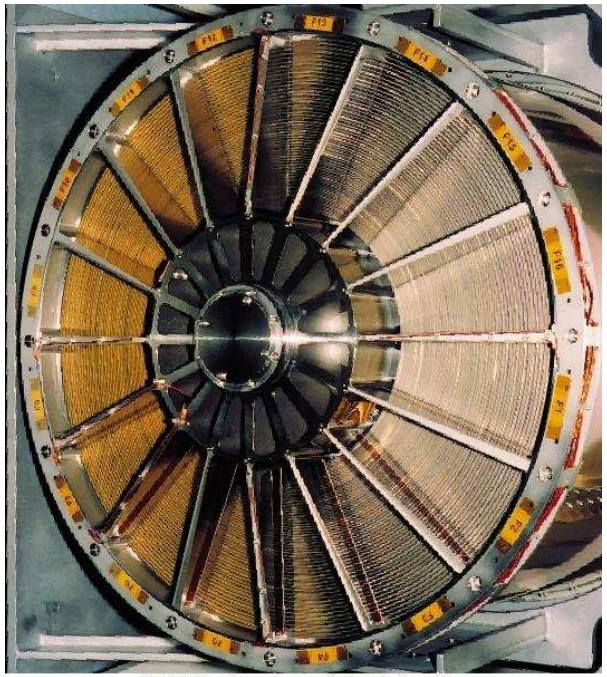

XMM-Newton mirrors during integration

Image courtesy of Dornier Satellitensysteme GmbH European Space Agency

Mirror manufacture

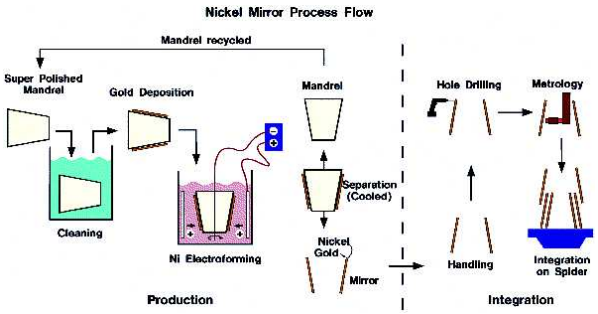

Recipe for making an X-ray mirror:

1. Produce mirror negative (“Mandrels”): Al coated with Kanigen nickel (Ni+10% phosphorus), super-polished [0.4 nm roughness]).
2. Deposit 250 nm Au onto Mandrel
3. Deposit 1 mm Ni onto mandrel (“electro-forming”, 10 μm/h)
4. Cool Mandrel with liquid N. Au sticks to Nickel
5. Verify mirror on optical bench.

Total production time of one mirror: 12 d, for XMM: 3×58 mirrors.

Mirror manufacture

Gold plastered mandrel for one of the XMM mirrors before electroforming the Ni shell onto the gold.

ESA picture 96.05.006-070

Mirror manufacture

. . . insertion of Mandrel into electroforming bath

ESA picture 96.12.002-016

Mirror manufacture

. . . and the mirror is done

ESA picture 96.12.002-093

XMM-Newton

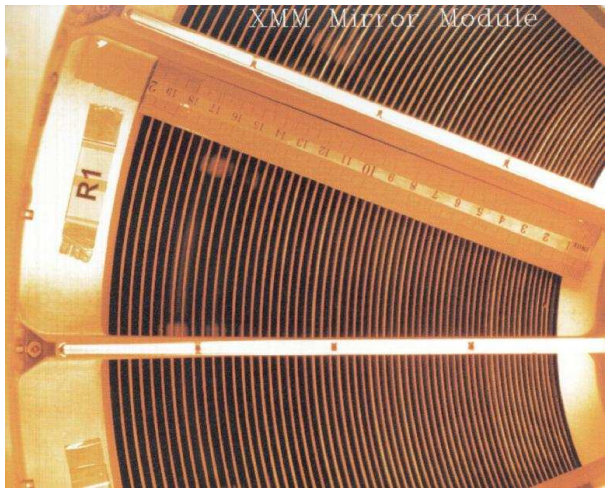

Top of the XMM mirrors:
3 mirror sets, each consisting of 58 mirrors,

- Thickness between 0.47 and 1.07 mm
- Diameter between 306 and 700 mm,
- Masses between 2.35 and 12.30 kg,
- Mirror-Height 600 mm
- Reflecting material: 250 nm Au.

photo: Kayser-Threde

The *XMM-Newton* Spacecraft (photo: ESA)

Semi-Conductors

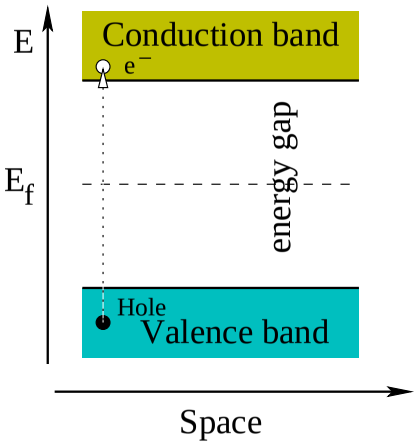

Semiconductors: separation of valence band and conduction band $\sim$1 eV (=energy of visible light).

Absorption of photon produces

$$N \sim \frac{h\nu}{E_{\text{gap}}} \qquad (5.10)$$

electron-hole pairs.

For Si: $E_{\text{gap}} = 1.12$ eV; 3.61 pairs created per eV photon energy [takes into account collective effects in semiconductor]

Note: band gap small $\Longrightarrow$ need cooling!

- optical light: $\sim$1 electron-hole pair
- X-rays (keV): $\sim$1000 electron-hole pairs

Problem: electron-hole pairs recombine immediately in a normal semiconductor $\Longrightarrow$ in practice, apply voltage to a “pn-junction” to separate electrons and pairs.

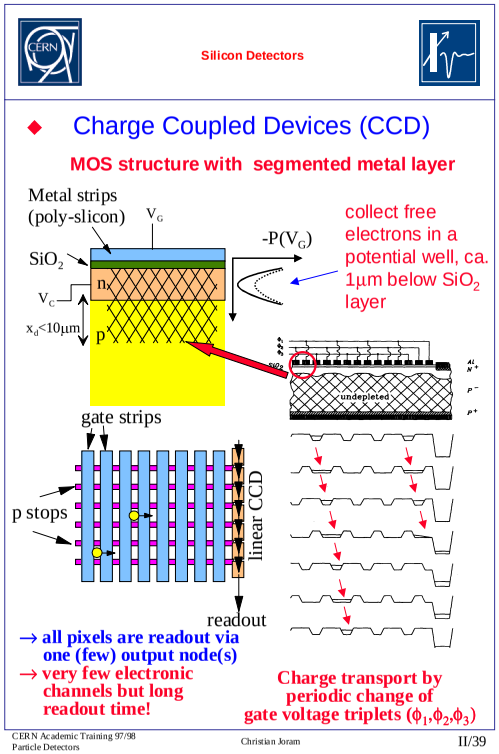

Backside Illuminated CCDs

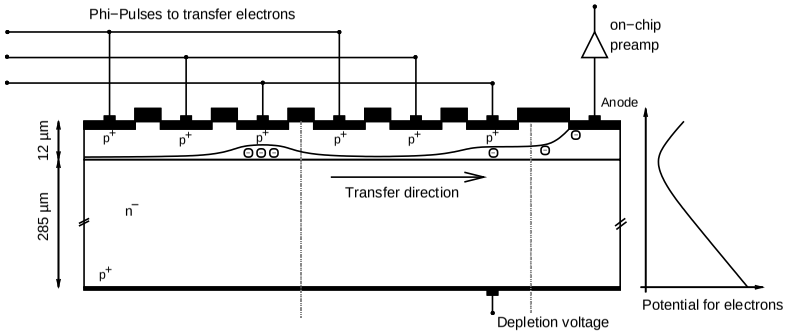

Schematic structure of the *XMM-Newton* EPIC pn CCD.

Problem: Infalling structure has to pass *through* structure on CCD surface $\Longrightarrow$ loss of low energy response, also danger through destruction of CCD structure by cosmic rays. . .

Solution: Irradiate the back side of the chip. Deplete whole CCD-volume, transport electrons to pixels via adequate electric field (“backside illuminated CCDs”)

XMM-Newton: EPIC-pn CCD

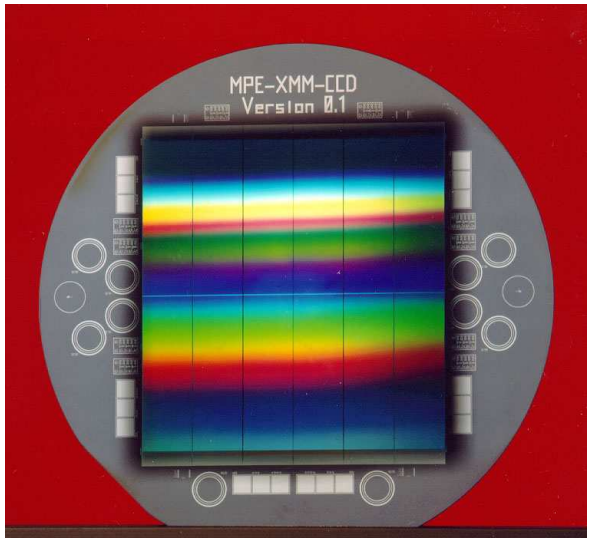

XMM-Newton: Array of individual backside illuminated CCDs on one Silicon wafer $\Longrightarrow$ requires extreme care during production

at the time of production one of the most complex Silicon structures ever made (diameter: 65.5 mm)

XMM-Newton: EPIC-pn CCD

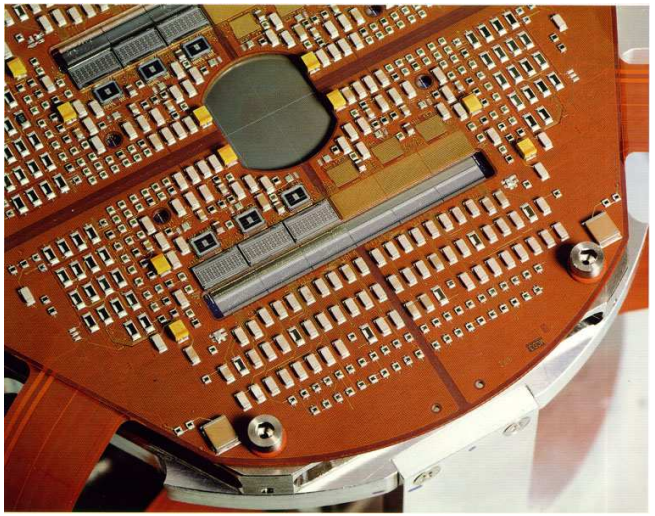

Backside of the EPIC-pn camera head

XMM-Newton: EPIC-pn CCD

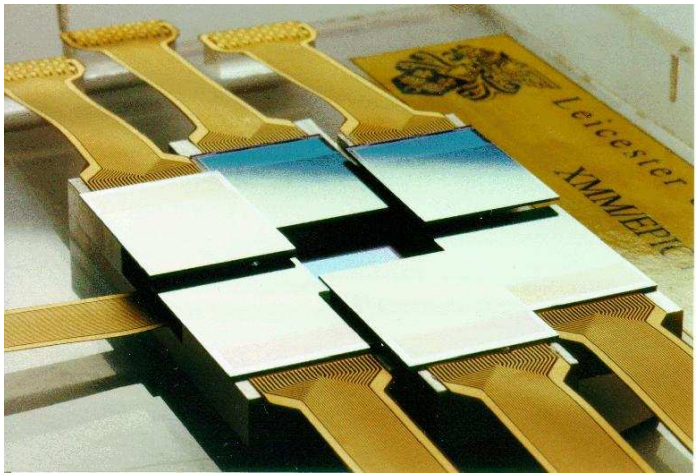

XMM-Newton (EPIC-MOS; Leicester): 7 single CCDs with 600 $\times$ 600 pixels, mounting is adapted to curved focal plane of the Wolter telescope.

Data Analysis

optical CCDs: mesure intensity $\Longrightarrow$ need *long* exposures

X-ray CCDs: measure individual photons $\Longrightarrow$ need fast readout

bright sources: several 1000 photons per second $\Longrightarrow$ readout in μs!

In X-rays: spectroscopy possible. Typical resolution reached today:

$$\frac{\Delta E}{E} = 2.355\sqrt{\frac{3.65\,\mathrm{eV}\cdot F}{E}} \tag{5.11}$$

with $F \sim 0.1 \Longrightarrow \sim 0.4\%$, so much better than gas detectors.

Energy $\propto$ number N of initial photoelectrons $\Longrightarrow$ Energy resolution (Poisson statistics!):

$$\frac{\Delta E}{E} \propto \frac{\Delta N}{N} = \frac{N^{1/2}}{N} = \frac{1}{N^{1/2}} \propto E^{-1/2} \tag{5.12}$$

For both optical and X-rays: sensitivity close to 100%

Si-based CCDs are currently the best available imaging photon detectors for optical and X-ray applications.

Data Analysis

Finite resolution of X-ray detectors has major implications for X-ray data analysis.

Mathematical description of the X-ray measurement process:

$$n_{\mathrm{ph}}(c) = \int_0^\infty R(c,E)\cdot A(E)\cdot F(E)\,dE \tag{5.13}$$

where

- $n_{\mathrm{ph}}(c)$: source count rate in channel c (counts s^{-1}),
- $F(E)$: photon flux density (ph cm^2 s^{-1} keV^{-1}),
- $A(E)$: effective area (units: cm^2),
- $R(c,E)$: detector response (probability to detect photon of energy E in channel c).

Data Analysis

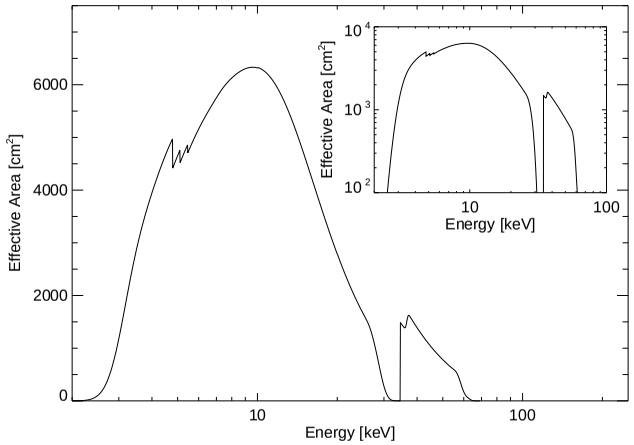

Effective Area of the Rossi X-ray Timing Explorer's Proportional Counter Array (Xe gas detector).

Data Analysis

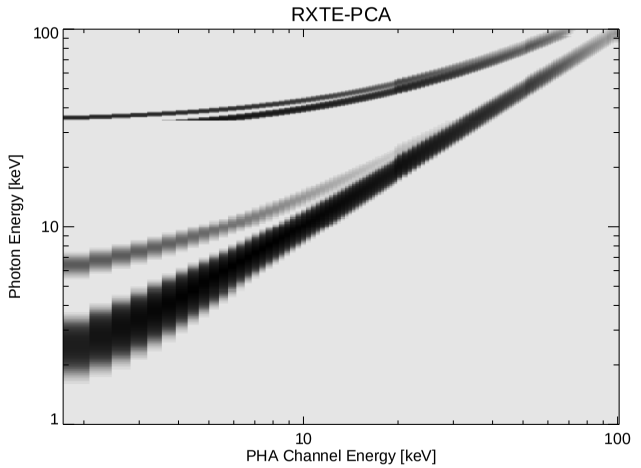

Response Matrix of the RXTE-PCA. Note the secondary peaks in the response caused by escaping Xe Kβ and Xe Lα photons.

Data Analysis

To analyze data: discretize Eq. (5.13):

$$S_{\mathrm{ph}}(c) = \Delta T \sum_{i=0}^{n_{\mathrm{ch}}} A(E_i) R(c,i) F(E_i) \Delta E_i \tag{5.14}$$

where $N_{\mathrm{ph}}(c)$: total source counts in channel c, ΔT: exposure time (s), x$A(E_i)$: effective area in energy band i (“ancilliary response file”, ARF), $R(c,i)$: response matrix (RMF), $F(E_i)$: source flux in band (E_i, E_{i+i}), ΔE_i: width of energy band.

Because of background $B(c)$ (counts), what is measured is

$$N_{\mathrm{ph}}(c) = S_{\mathrm{ph}}(c) + B(c) \tag{5.15}$$

So estimated source count rate is

$$\tilde{S}_{\mathrm{ph}}(c) = N_{\mathrm{ph}}(c) - B(c) \tag{5.16}$$

with uncertainty (Poisson!)

$$\sigma\tilde{S}_{\mathrm{ph}}(c) = \sqrt{\sigma N_{\mathrm{ph}}(c)^2 + \sigma B(c)^2} = \sqrt{N_{\mathrm{ph}}(c) + B(c)} \tag{5.17}$$

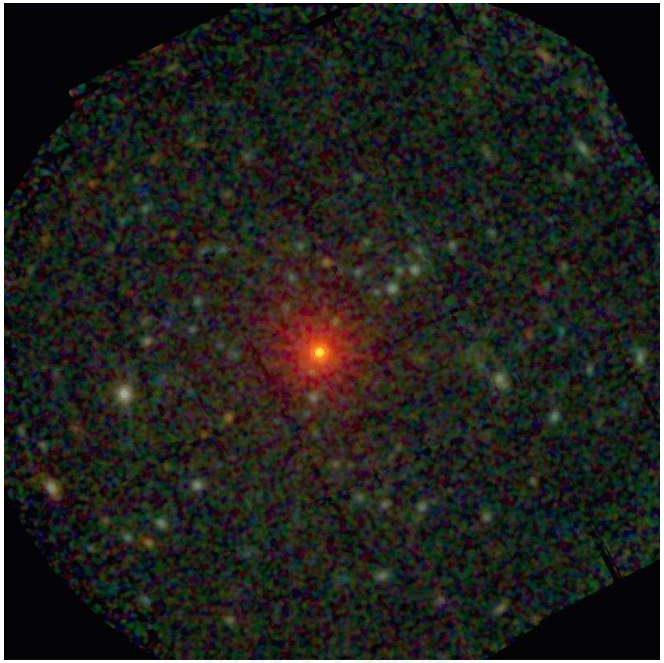

The isolated neutron star RX J0720.4-3125

Image courtesy of F. Haberl

European Space Agency

X

Data Analysis

To get physics out of measurement, need to find $F(E_i)$.

Big problem: In general, Eq. (5.14) is *not invertible*.

$\Longrightarrow$ χ^2-minimization approach

Use a model for the source spectrum, $F(E;\boldsymbol{x})$, where $\boldsymbol{x}$ vector of parameters (e.g., source flux, power law index, absorbing column,...), and calculate predicted model counts, $M(c;\boldsymbol{x})$, using Eq. 5.14).

Then form χ^2-sum:

$$\chi^2(\boldsymbol{x}) = \sum_c \frac{\left(\tilde{S}_{\mathrm{ph}}(c) - M(c;\boldsymbol{x})\right)^2}{\sigma\tilde{S}_{\mathrm{ph}}(c)^2} \tag{5.18}$$

Then vary $\boldsymbol{x}$ until χ^2 is minimal and perform statistical test based on χ^2 whether model $F(E;\boldsymbol{x})$ describes data.

Programs used: `XSPEC`, `ISIS`

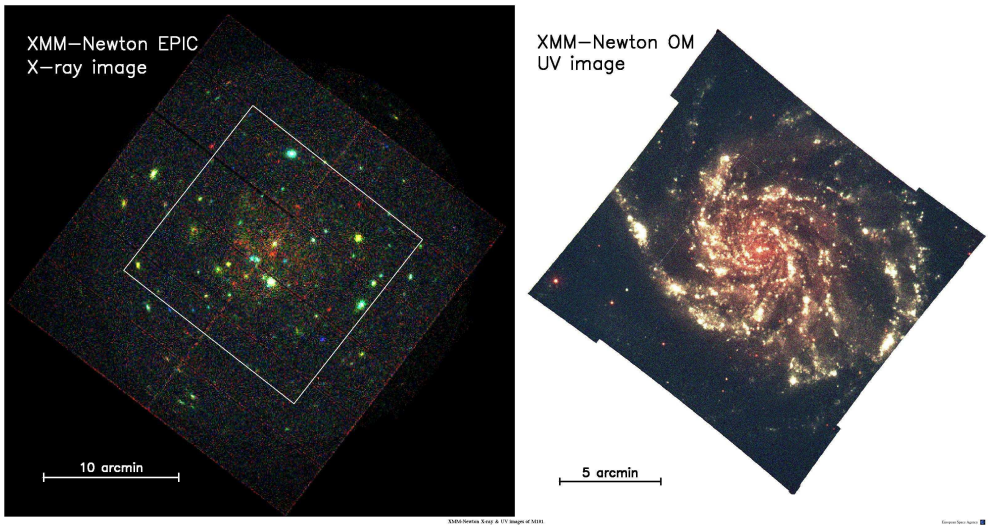

Point sources: Accreting stellar-mass systems in M101.

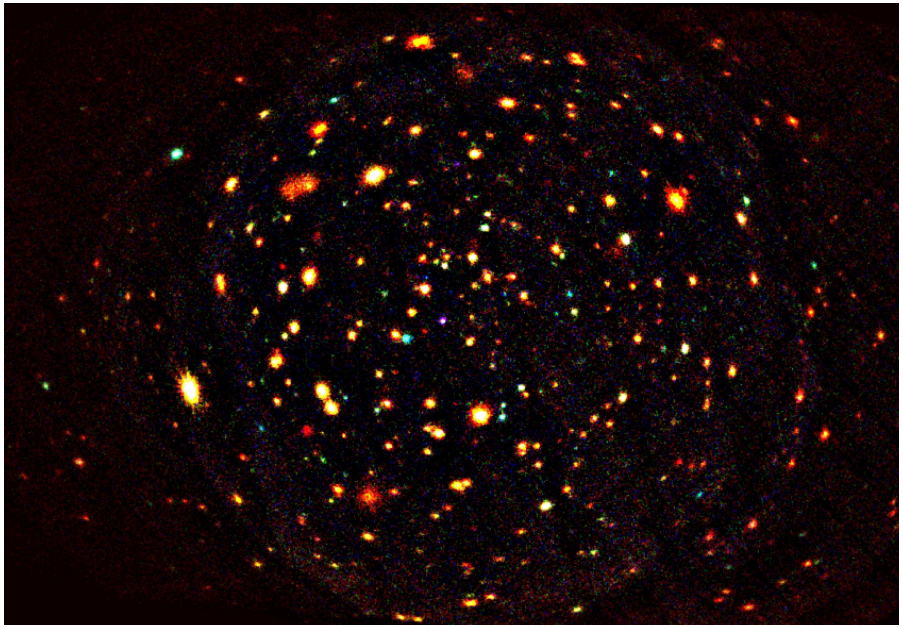

Lockman-Hole with *XMM-Newton*: The Universe is full of AGN!

Aschenbach, B., 1985, Rep. Prog. Phys., 48, 579